

Award Accounts

The Chemical Society of Japan Award for Creative Work for 2004

Development of New Fast Oxide Ion Conductor and Application for Intermediate Temperature Solid Oxide Fuel Cells

Tatsumi Ishihara

Department of Applied Chemistry, Faculty of Engineering, Kyushu University,
744 Motooka, Nishi-ku, Fukuoka 819-0395

Received November 21, 2005; E-mail: ishihara@cstf.kyushu-u.ac.jp

Solid Oxide Fuel Cell (SOFC) show great promise as new power generators with high efficiency. Decreasing the operating temperature is critically required for the further development of SOFC. This review introduces that oxide ion conductivity in the perovskite oxide of $LaGaO_3$, which was found by our group. $LaGaO_3$ doped with La and Mg exhibits the high oxide ion conductivity over a wide P_{O2} range; the value is higher than that of Y_2O_3-stabilized ZrO_2 by an order of magnitude. When $LaGaO_3$-based oxide was used as the electrolyte of SOFC, the power density could be improved greatly, in particular over the low-temperature range. In this study, the power generating property of LSGM using a thin film of $LaGaO_3$ is also introduced. The maximum power density of the cell using $LaGaO_3$-based oxide is as high as 0.6 W cm^{-2} at 773 K. This suggests that SOFC could be operable at temperature lower than 773 K.

1. Introduction

Oxide ions or proton-conducing oxides can be used for the electrolyte of fuel cells. Therefore, development of a high oxide ion or proton-conducting ceramics is a highly important subject. At present, the oxide ion conductors are mainly used for the electrolytes of solid oxide fuel cells (SOFCs). However, proton-conducting oxide is also an important class of such electrolytes. Up to now, fluorite oxides such as stabilized ZrO_2 or doped CeO_2 were mainly used as the electrolyte of fuel cells; however, there are other oxides which also exhibit the high oxide ion or proton conduction required for the electrolyte of fuel cells.[1] Among them, perovskite oxides of $LaGaO_3$ and $CaTiO_3$ (oxide ions), $BaCeO_3$ and $BaZrO_3$ (protons), perovskite-related oxide of $Ba_2In_2O_5$ (oxide ion), and the new crystal-phase oxides of La_2GeO_5[2] and $La_{10}Si_6O_{26}$[3,4] (oxide ion) are highly attractive for use as the electrolyte of SOFCs. The ionic conducting properties in these oxides have been investigated extensively. Perovskite oxide of $LaMnO_3$ or $LaCoO_3$ is generally considered as the active electrode catalyst for SOFC. However, perovskite oxide is also an extremely important crystal structure for the oxide ion conductor for the electrolyte of SOFC. In this review, the oxide ion conductivity in $LaGaO_3$-based oxide doped with La and Sr is introduced and the power generating property of SOFC using $LaGaO_3$-based oxide is also demonstrated.

2. Crystal Structure and Oxide Ion Conductivity in Perovskite Oxide

In the case of oxide ion conductors, the fluorite oxide consisting of tetravalent cation exhibits superior oxide ion conductor properties. In particular, Y_2O_3-stabilized ZrO_2 is popularly used. Since a large part of the non-fluorite ion conductor has a perovskite structure, the crystal structure of perovskite oxide should be briefly introduced. The perovskite-type oxides based on the general formula ABO_3 comprise a rich family of compounds with important applications in solid oxide fuel cells, ferroelectric, super-conducting materials, oxidation catalysis, etc. This is because the total charge on A and B (+6) can be achieved by the combinations of $1+5$, $2+4$, and $3+3$, and also in more complex ways as in $Pb(B'_{1/2}B''_{1/2})O_3$, where $B' = Sc$ or Fe and $B'' = Nd$ or Ta, or $A'_{1/2}A''_{1/2}TiO_3$ where $A' = Li$ or Na and $A'' = La$, Pr, etc. Also, there are many compounds which are polymorphic to a perovskite structure such as the K_2NiF_4 structure; defect perovskite oxide. As illustrated in Fig. 1, the ideal perovskite structure is cubic, with 12-coordinated large cations of A and 6-coordinated small cations of B. From the geometry of the structure, it follows, that for the ideal structure, there is the following relation between the radii of A, B, and O ions.

$$r_A + r_O = \sqrt{2}(r_B + r_O). \quad (1)$$

Actually the cubic perovskite structure or slightly deformed variants of it are found for ions which do not obey this relation exactly, and this was expressed by introducing a "tolerance factor," t.

$$t = \frac{r_A + r_O}{\sqrt{2}(r_B + r_O)}. \quad (2)$$

Namely, t close to 1 means the structure is closer to the ideal in

Published on the web August 7, 2006; doi:10.1246/bcsj.79.1155

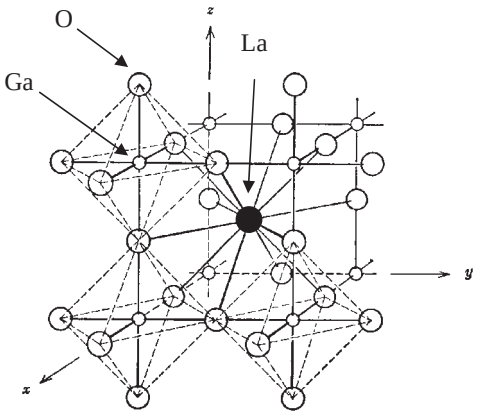

Fig. 1. Ideal perovskite structure.

geometry. Due to the high stability of crystal structure and the variety in included cations, perovskite oxide can accommodate a large amount of oxygen deficiency. Consequently, a large variety in properties has also been found on this structure oxide. Namely, an oxide having perovskite structure exhibits the wide range of electronic conducting property from the highly electronic conductivity at a famous super-conducting oxide of $Ba_3Cu_2YO_7$ to that of a dielectric oxide such as $BaTiO_3$. Therefore, a unique electrical conducting property is also expected for this oxide. Recently, some interesting reports on ionic conductivity in perovskite oxide were reported, i.e., high-temperature proton conduction in doped $BaCeO_3$ or $BaZrO_3$ or high lithium conduction in $La(Li)TiO_3$. Therefore, oxide with perovskite structure is a highly important group for developing a new ion conductor.

Although the oxide with perovskite structure is anticipated to be a superior oxide ion conductor, typical perovskite oxides such as $LaCoO_3$ and $LaFeO_3$ are known as a famous mixed electronic and oxide ionic conductors. Therefore, these mixed conducting perovskite oxides can be used as the cathode catalysts for SOFC or oxygen permeating membranes. For the electrode catalysis, not only high electrical conductivity but also high catalytic activity is required. $LaCoO_3$-based oxide exhibits the high activity for oxygen dissociation and so the high activity to the oxidation reaction of hydrocarbon, the value is comparable with that of Pt catalyst, a famous oxidation catalyst.[5] In addition, $LaCoO_3$ doped with Sr on La sites is a famous high electrical conductor. However, the oxide ion conductivity in this $LaCoO_3$ is higher than that in 8 mol % Y_2O_3-stabilized ZrO_2, a typical oxide ion conductor. Therefore, development of a high oxide ion conductor is expected from the perovskite oxide studies. Now the large majority of perovskite oxides exhibiting the oxide ion conduction are classified as mixed conductors, which show both electronic and oxide ionic conduction.

Takahashi and Iwahara have done pioneering work on oxide ion conductivity in perovskite-type oxides.[6] They reported the fast oxide ion conductivity in Ti- and Al-based perovskite oxide. Figure 2 shows the oxide ion conductivity in some perovskite oxide reported by Takahashi and Iwahara.[6] This figure makes it clear that Al- or Mg-doped $CaTiO_3$ exhibits the highest conductivity. Therefore, Takahashi and Iwahara investigated the oxide ion conductivity in $CaTiO_3$ in detail. On the other

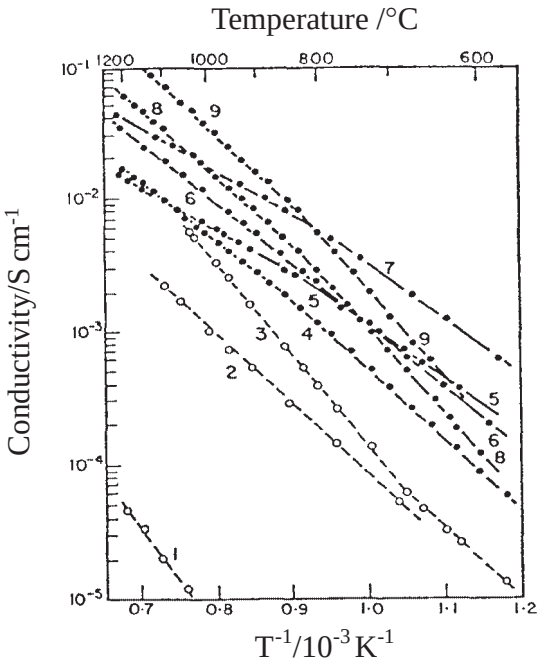

Fig. 2. Temperature dependence of oxide ion conductivity in some perovskite oxide. Number in figure corresponds to the following sample; (1) $LaAlO_3$, (2) $CaTiO_3$, (3) $SrTiO_3$, (4) $La_{0.7}Ca_{0.3}AlO_3$, (5) $La_{0.9}Ba_{0.1}AlO_3$, (6) $SrTi_{0.9}Al_{0.1}O_3$, (7) $CaTi_{0.95}Mg_{0.05}O_3$, (8) $CaTi_{0.5}Al_{0.5}O_3$, (9) $CaTi_{0.9}Al_{0.3}O_3$.

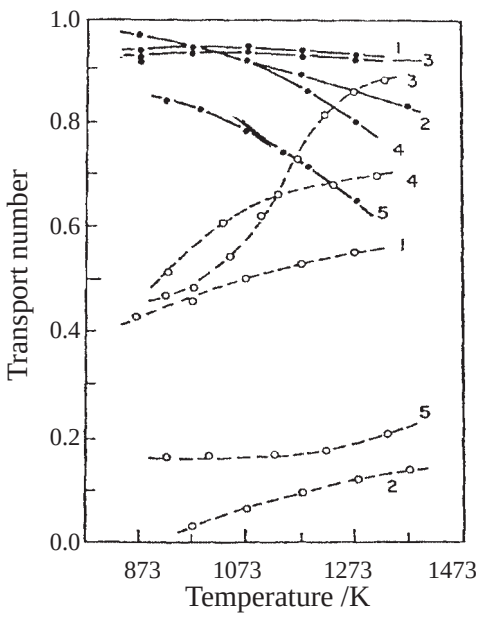

Fig. 3. Transport number of some perovskite oxide estimated with H_2–O_2 gas concentration cell. Number in figure corresponds to the same one in Fig. 2 and broken line and solid line are the data obtained by O_2–air and O_2–humidified H_2 cells, respectively.

hand, Figure 3 shows the transport number estimated with H_2–O_2 gas concentration cell. Although the high transport number of oxide ion is obtained on $CaTi_{0.95}Mg_{0.05}O_3$ at intermediate temperature, Ca-doped $LaAlO_3$ is another attractive candidate

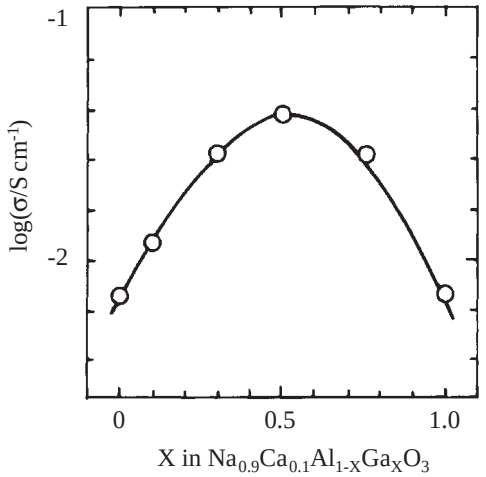

Fig. 4. Oxide ion conductivity in $NdAlO_3$ at 1123 K as a function of Ga amount.

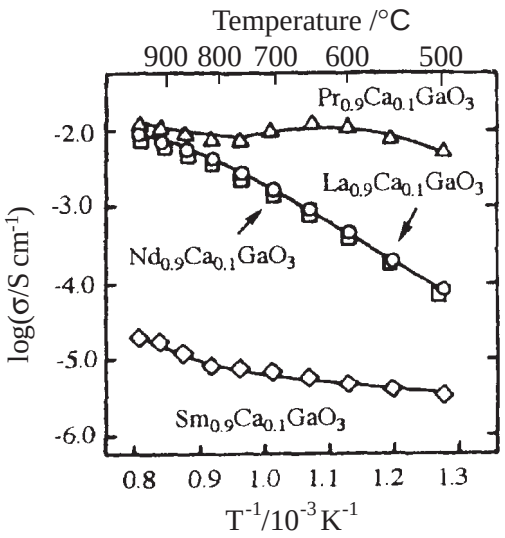

Fig. 5. Arrhenius plots of the electrical conductivity of Ca-doped $LnGaO_3$ (Ln = La, Pr, Nd, and Sm).

as a oxide ion conductor, since no electronic conduction appears in reducing atmosphere and transport number is higher than 0.9 over the entire temperature range, as shown in Fig. 3.

After the report of Takahashi and Iwahara,[6] many researchers have investigated the oxide ion conductivity in $LaAlO_3$-based oxide. However, the reported oxide ion conductors with perovskite structure exhibited lower ionic conductivity than that of YSZ. In the conventional study on perovskite oxide of ABO_3, researchers have believed that the electric or dielectric property was strongly dependent on B site cations. However, a migrating oxide ion will have to pass through the triangle space consisting of two large A and one small B site cations in the crystal lattice. Theoretical calculations suggest that the enlargement of the size of this triangle space is important for improving the migration of oxide ion.[7] Therefore, the ionic size of the A site cation seems to influence greatly the oxide ion conductivity. Based on these concepts, we studied first the oxide ion conductivity in $NdAlO_3$ doped with Ga at Al sites.[8] The addition of Ga^{3+}, a larger ion than Al^{3+}, to B sites of $NdAlO_3$ is effective for improving the oxide ion conductivity.[9] Figure 4 shows the oxide ion conductivity at 1123 K as a function of Ga amount. In accordance with the prediction, oxide ion conductivity increased with increasing amount of Ga and it attained the maximum ($\log(\sigma/\mathrm{S\,cm^{-1}}) = -1.5$ at 1223 K when 50 mol % Ga was doped at Al sites in $LaAlO_3$. Since no oxygen vacancy is formed by doping Ga^{3+} due to the valence number being the same, the improved oxide ion conductivity is brought about by the improved mobility of oxide ion. Although the high oxide ion conductivity was obtained on $Nd_{0.9}Ca_{0.1}Al_{0.5}Ga_{0.5}O_3$, the oxide ion conductivity of this compound is still lower than that of YSZ. However, we expect that the higher oxide ion conductivity will be obtained on the perovskite oxide with the larger unit lattice size. $LaGaO_3$ has quite a large unit lattice size judging from the JCPDS data base (Card No. 24-1104); therefore, higher oxide ion conductivity in Ga-based perovskite-type oxide is predicted.

3. $LaGaO_3$-Based Oxide Doped with Sr and Mg (LSGM) as a New Oxide Ion Conductor

Since $Nd_{0.9}Ca_{0.1}GaO_3$ also exhibits oxide ion conduction, oxide ion conductivity in Ga-based perovskite oxide was investigated. Arrhenius plots of the electrical conductivity of Ca-doped $LnGaO_3$ (Ln = La, Pr, Nd, and Sm) are shown in Fig. 5.[10] It is obvious that the oxide ion conductivity strongly depends on the cations for A site, which is similar to the case of Al-based oxide. The electrical conductivity increased in the following order, Pr > La > Nd > Sm. The electrical conductivity of all Ga-based perovskite oxides is almost independent of the oxygen partial pressure. Therefore, it is expected that the oxide ion conduction will be dominant in all Ga-based perovskite oxides. Since the electrical conductivity of $LaGaO_3$ is independent of oxygen partial pressure in the widest range among the examined oxides, the oxide ion conductivity in $LaGaO_3$ is the most promising among these Ga-based oxides.

Doping a lower valence cation generally forms the oxygen vacancies due to the electric neutrality; the oxide ion conductivity will increase with increasing the amount of oxygen vacancies. Therefore, doping alkaline earth cations to La sites was investigated and the oxide ion conductivity is shown in Fig. 6.[11] The electrical conductivity in $LaGaO_3$ depends strongly on the alkaline earth cations doped at La sites and increased in the following order Sr > Ba > Ca. Therefore, the strontium is the most suitable dopant for La sites in $LaGaO_3$. Theoretically, increasing amount of Sr will increase the amount of oxygen vacancy and the oxide ion conductivity will be elevated with increasing Sr amount. However, the solid solubility of Sr into La sites of $LaGaO_3$ is poor and the secondary phases $SrGaO_3$ or La_4SrO_7 form when the amount of Sr becomes higher than 10 mol %. Therefore, the amount of oxygen vacancy introduced by La site doping is not large.

In case of the perovskite oxide, oxygen vacancy can be also introduced by doping Ga sites in addition to La sites. In the conventional studies, this so-called "double doping" of aliovalent cations is limited. The effects of dopant on Ga sites of $La_{0.9}Sr_{0.1}GaO_3$ were studied for further improvement of the electrical conductivity. It is found that doping Mg is highly effective for increasing the conductivity, since additional oxide ion vacancies are formed. The oxide ion conductivity is further

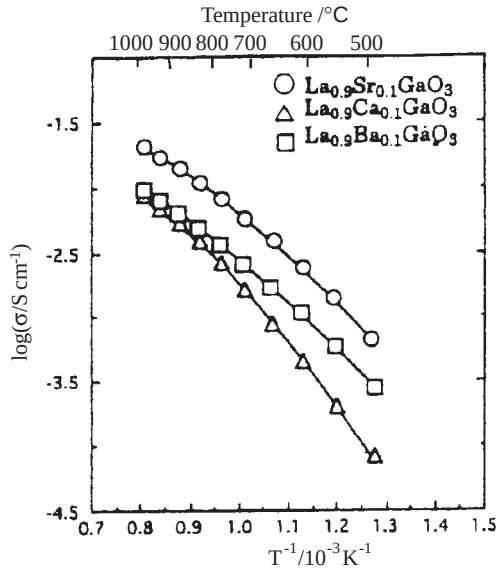

Fig. 6. Effects of alkaline earth cations in La site on the oxide ion conductivity in $LaGaO_3$.

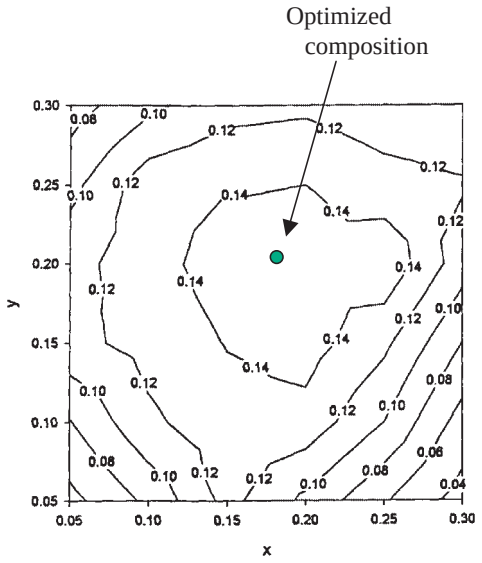

Fig. 7. Contour plot of the conductivity in $La_{1-X}Sr_XGa_{1-Y}Mg_YO_3$ at 1073 K.

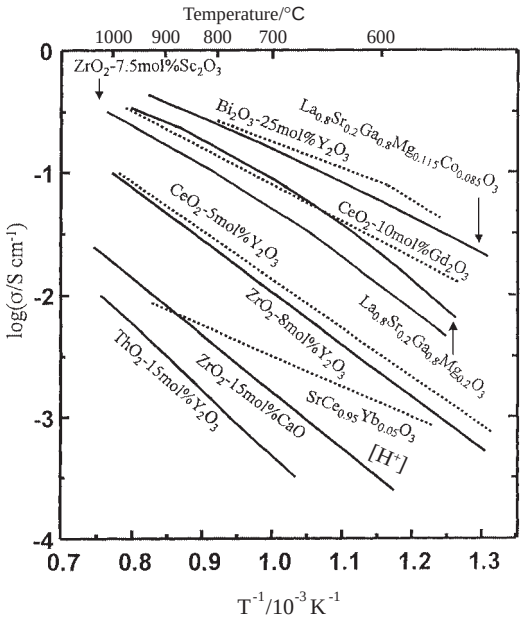

Fig. 8. Comparison of the oxide ion conductivity in doubly doped $LaGaO_3$ with the conventional oxide ion conductors.

increased by increasing the amount of doped Mg; it attained the maximum at 20 mol % Mg doped for Ga sites. The lattice parameter also increases by doping Mg for Ga sites, since the ionic radius of Mg is larger than that of Ga. The solid solubility of Sr into $LaGaO_3$ lattice seems to reach a limit around 10 mol % without Mg; however, it increases up to 20 mol % by doping Mg for Ga site. This enlargement in the limit of Sr solid solution in La sites is also reported by Majewski et al.[12] This seems to be due to the enlarged crystal lattice. In any case, the authors found that the highest oxide ion conductivity in $LaGaO_3$-based oxide is obtained at the composition of $La_{0.8}Sr_{0.2}Ga_{0.8}Mg_{0.2}O_3$.[13]

After our report,[11] oxide ion conductivity in $LaGaO_3$-based oxide was investigated by several groups and various cations were examined as a dopant for $LaGaO_3$-based oxides.[14] Huang and Petric investigated the oxide ion conductivity in various compositions and expressed the oxide ion conductivity in contour maps.[15] It was reported that the highest oxide ion conductivity was obtained at the composition of $La_{0.8}Sr_{0.2}Ga_{0.85}Mg_{0.15}O_3$. On the other hand, Huang et al. also investigated the oxide ion conductivity in $LaGaO_3$ doped with Sr and Mg at various compositions. Figure 7 shows the contour plot of the conductivity at 1073 K.[16] The optimized composition in $La_{1-X}Sr_XGa_{1-Y}Mg_YO_3$ with the highest conductivity $\sigma = 0.17\,S\,cm^{-1}$ is $X = 0.2$, $Y = 0.17$.[16] However, the optimized composition among the three groups is close and the optimized composition in Sr- and Mg-doped $LaGaO_3$ exists between $Y = 0.15$ to 0.2 in $La_{0.8}Sr_{0.2}Ga_{1-Y}Mg_YO_3$.

Figure 8 shows the comparison of oxide ion conductivity of doubly doped $LaGaO_3$ with the conventional oxide ion conductors.[13] It is obvious that the oxide ion conductivity in $La_{0.8}Sr_{0.2}Ga_{0.8}Mg_{0.2}O_3$ is higher than the typical conductivity of ZrO_2- or CeO_2-based oxides and somewhat lower than those of Bi_2O_3-based oxides. It is well-known that electronic conduction is dominant in CeO_2- or Bi_2O_3-based oxides under a reducing atmosphere; furthermore, thermal stability is not satisfactory in Bi_2O_3-based oxides. In contrast, $La_{0.8}Sr_{0.2}Ga_{0.8}Mg_{0.2}O_3$ exhibits wholly ionic conduction from $P_{O2} = 10^{-20}$ to 1 atm. Therefore, doubly doped $LaGaO_3$ perovskite oxide shows great promise as the solid electrolyte of fuel cell and oxygen sensor.

Since the minor carrier of electron and hole determines the chemical leakage of oxygen when the oxide ion conductor is applied for the electrolyte of SOFC, performance of electron and hole conduction is an important subject. Performance of hole and electron conduction and transport number of oxide ion in $LaGaO_3$-based oxide were measured by the polarization method by Baker et al.,[17] Yamaji et al.,[18] and Kim et al.[19] Figure 9 shows the estimated hole and electron conduction in LSGM as a function of oxygen partial pressure.[19] It is seen

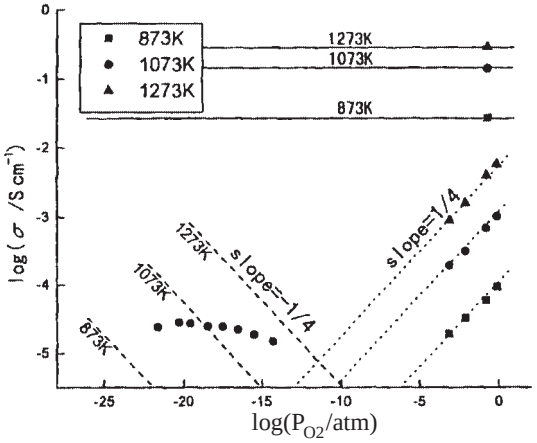

Fig. 9. Estimated hole and electron conduction in LSGM as a function of oxygen partial pressure.

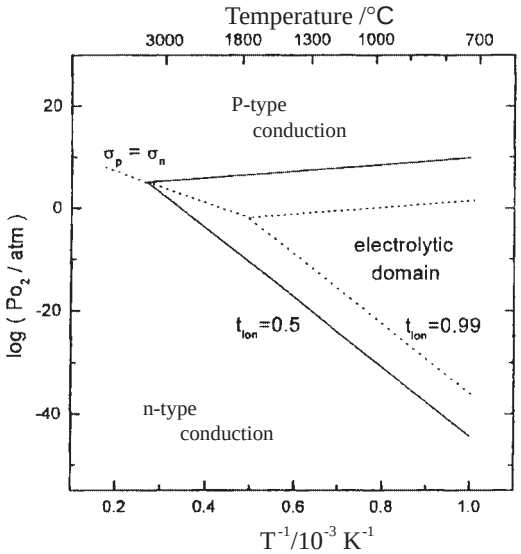

Fig. 10. Boundaries of the electrolytic domain of $La_{0.9}Sr_{0.1}Ga_{0.8}Mg_{0.2}O_3$ in the plane of $\log(P_{O2}/\text{atm})$ versus reciprocal temperature.

that P_{O2} dependence of hole and electron is $P_{O2}{}^{1/4}$ and $P_{O2}{}^{-1/4}$, respectively, and well obeys the Hebb–Wagner theory. This polarization method clearly suggests that $LaGaO_3$-based oxide exhibits almost pure oxide ion conduction over a wide range of oxygen partial pressure ($10^5 > P_{O2} > 10^{-25}$ atm). Compared with CeO_2-based oxide or Bi_2O_3 oxide, this is a remarkable advantage of this $LaGaO_3$-based oxide and the stability against the reduction corresponds to that of ZrO_2-based oxide. Consequently, it can be said that $LaGaO_3$-based oxide is highly promising as an electrolyte, particularly if compared with ceria-based oxide. Kim et al.[19] also investigated the temperature dependence of hole and electronic conductivity in $La_{0.9}Sr_{0.1}Ga_{0.8}Mg_{0.2}O_3$ with the polarization method. Figure 10 shows the evaluated boundaries of the electrolytic domain of $La_{0.9}Sr_{0.1}Ga_{0.8}Mg_{0.2}O_3$ in the plane of $\log(P_{O2}/\text{atm})$ versus reciprocal temperature. The lower boundary of the electrolytic domain (defined as $t_{ion} > 0.99$) for LSGM is 10^{-23} atm at 1273 K. This is even lower than that of CaO-stabilized ZrO_2 and that of YSZ. Consequently, it is clear that the electrolytic domain covers the P_{O2} range required for SOFC and that this LSGM could be used for the electrolyte of SOFC.

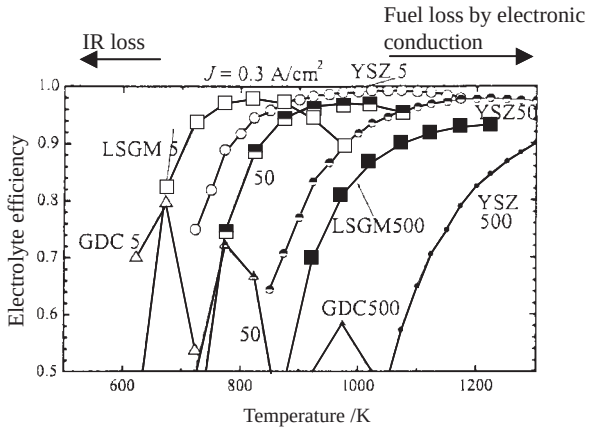

Fig. 11. Efficiency loss at selected values of thickness and at a current density of 0.3 A cm^{-2} in YSZ, Gd-doped CeO_2 (GDC), and LSGM.

Yokokawa et al. estimated the electrolyte efficiency when LSGM is used for the electrolyte of SOFC.[20] Electrolyte efficiency is given by a function of fuel utilization for the power generation and an internal resistance.[20] When the thickness of the electrolyte became thinner, chemical leakage of oxygen due to the electronic conduction became significant and the fuel consumption without generating electronic power also became significant resulting in the decreased electrolyte efficiency. On the other hand, with increasing thickness of electrolyte, the internal resistance of the cell increases resulting in the decreased electrolyte efficiency. Consequently, it is easily understood that some optimum thickness should exist for each electrolyte provided the operating temperature and the current density are fixed.

Figure 11 compares the efficiency loss at selected values of thickness and at a current density of 0.3 A cm^{-2} in YSZ, Gd-doped CeO_2(GDC), and LSGM.[20] The efficiency loss in the electrolyte increases rapidly with lowering temperature due to the Arrhenius-type behavior of the ionic conductivity. In order to achieve a high power density, it is essential to fabricate a thin film. Although the ionic conductivity of YSZ is small compared with those in GDC and LSGM, sufficiently high power density is successfully achieved by using a 5–10 μm thick YSZ at a low temperature of 800–1000 K. However, application of YSZ for the cell operating at an even lower temperature is difficult, since the IR loss becomes significant. On the other hand, the efficiency loss by consumption of fuel due to the electrochemically leaked oxygen is significant in the case of GDC. Although the transport number of oxide ion increased with decreasing operating temperature, the efficiency is not sufficiently high, as seen in Fig. 11. Therefore, ceria-based oxide is not appropriate as the electrolyte for SOFC operating at high temperature; however, doped ceria, in particular, Gd-doped ceria, becomes attractive because of the high oxide ion conductivity. LSGM exhibits the high oxide ion (as shown in Fig. 8) and the low electronic conductivity. Consequently, the efficiency on this oxide is comparable with that of YSZ, but the temperature at the highest efficiency becomes

lower than that of YSZ, as seen in Fig. 11. If the thickness of LSGM is 5 μm, then the highest efficiency can be achieved around 700 K. Therefore, LSGM is expected to be a potential electrolyte for SOFC operating at 600–800 K. Based on these aspects, the applications of LSGM for the electrolyte of SOFC are continuing at present.

4. Application of LSGM for the Electrolyte of SOFC

In order to achieve the high power density of fuel cells at an intermediate temperature, one needs not only highly ionic conductors but also highly active electrodes. Applications of LSGM for the electrolyte of fuel cells were investigated. Figure 12 shows the temperature dependence of the maximum power density and the open circuit potential (OCV) of the cell with $Sm_{0.5}Sr_{0.5}CoO_3$ cathode and Ni anode. It is seen that open circuit potential (OCV) increased with decreasing temperature; results are in good agreement with the theoretical values which are estimated by the Nernst equation. On the other hand, the power density was improved by using $Sm_{0.5}Sr_{0.5}CoO_3$ for cathodes at all temperatures examined. The maximum power density is higher than 1.0 and 0.1 W cm^{-2} at 1273 and 873 K, respectively in spite of the 0.5 mm thickness electrolyte. Goodenough and co-workers also investigated the application of $LaGaO_3$-based oxide for the electrolyte of fuel cell.[21] A

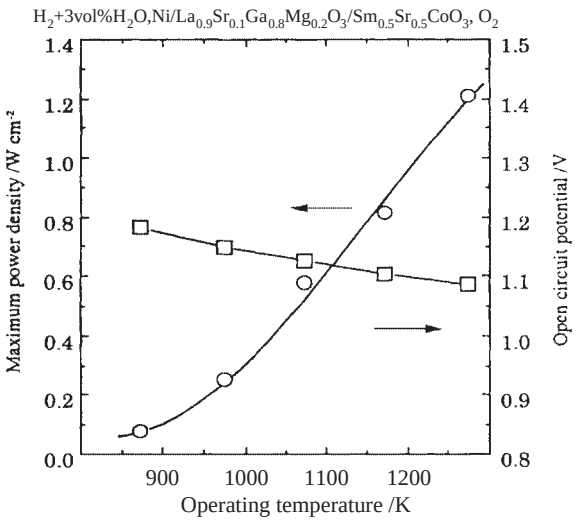

Fig. 12. Temperature dependence of the maximum power density and the open circuit potential (OCV) of the cell with $Sm_{0.5}Sr_{0.5}CoO_3$ cathode and Ni anode. Thickness of the electrolyte was 0.5 mm.

similar large power density is reported at an intermediate temperature with $La_{0.6}Sr_{0.4}CoO_3$ cathode and Ni–La-doped CeO_2 cermet anode. Due to such high power density, LSGM is attracting much interest as an electrolyte of intermediate temperature SOFC.

The reactivity of this $LaGaO_3$ oxide has been also investigated by several groups. The reactivity of $LaGaO_3$-based oxide[22] with $La(Sr)CoO_3$ perovskite oxide or Pt electrode[23] is important. In particular, platinum seems to easily react with gallium oxide to reduce Ga^{3+} to Ga^{+}, which is volatile. Therefore, for the practical application of this material for the electrochemical devices such as fuel cells, one should pay attention to the choice of the electrode material and/or its conditions of use such as temperature or atmosphere.

The thermal expansion property is another important subject for the application of fuel cells. Hayashi et al.[24] and the authors reported the thermal expansion properties of LSGM. The thermal expansion is increased with increasing the dopant amount. Anomalies of thermal expansion for $LaGaO_3$ and $La_{0.9}Sr_{0.1}GaO_3$ are observed around 400 K and these can be assigned to the phase transition from orthorhombic to rhombohedral. On the other hand, Sr- and Mg-doped materials show the monotonic expansion; the estimated average thermal expansion coefficient is around 11.5×10^{-6} K^{-1} in the temperature range from 298 to 1273 K. Therefore, the average thermal expansion coefficient is slightly larger than but close to that of Y_2O_3-stabilized ZrO_2.

The diffusivity in oxide ions in LSGM was further studied with ^{18}O tracer diffusion measurements.[25] LSGM exhibits the large diffusion coefficient and this large diffusion coefficient could originate from the high mobility of these oxide ions comparing with the diffusion coefficient of fluoride oxide (Table 1). Therefore, we consider that the perovskite structure has a large free volume in lattice and this large free volume could allow the high diffusivity of oxide ion, resulting in the high oxide ion conductivity.

In summary, $LaGaO_3$ doped with Sr and Mg for La and Ga sites are likely to be useful electrolytes for the intermediate temperature SOFC.

5. Transition Element Doping Effects on Oxide Ion Conductivity in $LaGaO_3$-Based Oxides

In this section, the effects of dopant on the oxide ion conductivity in $LaGaO_3$-based oxides are described. In order to improve the oxide ion conductivity, several groups have already investigated the effects of the various cation dopants on oxide ion conductivity in $LaGaO_3$-based oxides. It is gen-

Table 1. Comparison of Mobility of Oxide Ion in Selected Fluorite and LSGM Oxide at 1073 K[a)]

	D_t/cm^2 s^{-1}	Ea/eV	δ	$[V_O^{\bullet\bullet}]$/cm^{-3}	D/cm^2 s^{-1}	μ/cm^2 V^{-1} s^{-1}	Ref.
$Zr_{0.81}Y_{0.19}O_2$	6.2×10^{-8}	1.0	0.10	2.95×10^{21}	1.31×10^{-6}	1.41×10^{-5}	Kilner et al.
$Zr_{0.858}Ca_{0.142}O_2$	7.54×10^{-9}	1.53	0.142	4.19×10^{21}	1.06×10^{-7}	1.15×10^{-6}	Simpson et al.
$Zr_{0.85}Ca_{0.15}O_2$	1.87×10^{-8}	1.22	0.15	4.43×10^{21}	2.49×10^{-7}	2.69×10^{-6}	Kingery et al.
$Ce_{0.9}Gd_{0.1}O_2$	2.7×10^{-8}	0.9	0.05	1.26×10^{21}	1.08×10^{-6}	1.17×10^{-5}	Kilner et al.
LSGM(9182)	3.24×10^{-7}	0.74	0.15	2.52×10^{21}	6.40×10^{-6}	6.93×10^{-5}	this work
LSGM(8282)	4.13×10^{-7}	0.63	0.20	3.34×10^{21}	6.12×10^{-6}	6.62×10^{-5}	this work

a) D_t; Tracer diffusion coefficient, Ea; Activation energy, δ; Oxygen deficiency, $[V_O^{\bullet\bullet}]$: Oxygen vacancy concentration, D; Self diffusion coefficient, μ; mobility.

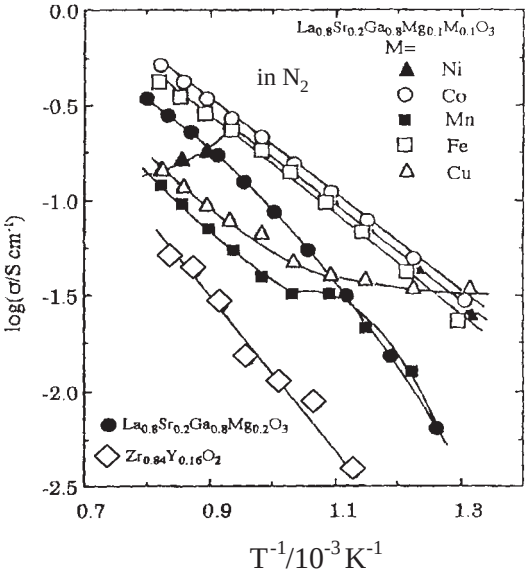

Fig. 13. Arrhenius plot of electrical conductivities of the $LaGaO_3$-based oxides doped with some transition-metal cations for Ga site.

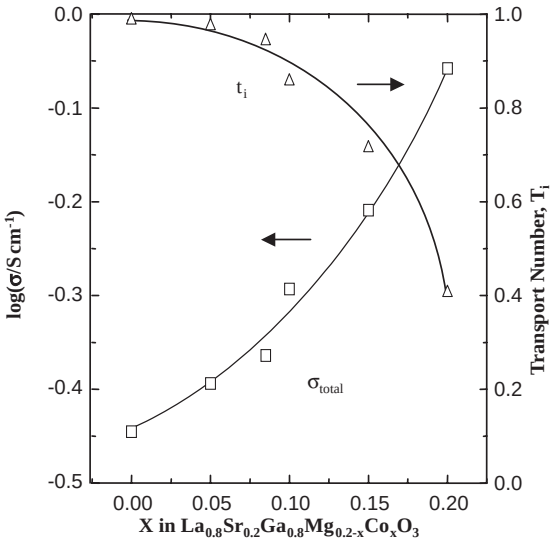

Fig. 14. Electrical conductivity of Co-doped LSGM at 1273 K, $P_{O2} = 10^{-5}$ atm and the transport number of oxide ion at 1273 K as a function of Co content.

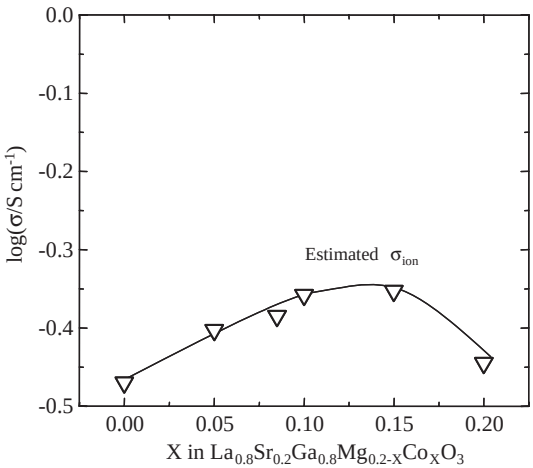

Fig. 15. Oxide ion conductivity estimated from the transport number and the total conductivity.

erally believed that doping transition-metal cations such as Co, Ni, or Fe enhances the electron or the hole conduction. Therefore, doping these cations is not desirable from the viewpoint of an oxide ion-conducting electrolyte. However, it is found that oxide ion conductivity increased by doping Co without any decreasing the transport number of oxide ion,[26] if the amount of Co is smaller than 10 mol %. In this section, the effect of the transition metal doping on oxide ion conductivity is briefly summarized.

Baker et al. investigated the effects of transition metals Cr and Fe on the oxide ion conductivity of $LaGaO_3$-based oxide.[27] It was reported that doping Cr or Fe adding in Ga sites induces the hole conduction in $LaGaO_3$-based oxides, resulting in the decreased stability against reduction. On the other hand, we found that doping a small amount of transition metal, in particular Co or Ni, is effective for increasing the oxide ion conductivity in LSGM.[27]

Figure 13 shows the Arrhenius plot of electrical conductivities of the $LaGaO_3$-based oxides doped with some transition-metal cations for Ga sites. It was observed that the conductivity is improved by doping Co and Fe, and is lowered by doping Cu and Mn. In the case of Ni, the conductivity decreased at temperatures higher than 1073 K, whereas above 973 K, it increased with increasing temperature. Such a decrease in conductivity in spite of increasing temperature may result from the significant electronic conductivity change caused by the thermal reduction of Ni. From the P_{O2} dependence of electrical conductivity, n-type conduction greatly enhanced by doping Mn and Ni, and p-type conduction increases by doping Cu. Kharton et al. also investigated the effects of transition-metal dopant on the oxide ion conductivity in $LaGa_{0.8}Mg_{0.2}O_3$.[28] Although the amount of doped transition metal is much larger, i.e., 40 mol % for Ga sites, they also reported that doping Mn and Cr decreases the oxide ion conductivity. However, Thangadurai et al. reported that the $La_{0.9}Sr_{0.1}Ga_{0.8}Mn_{0.2}O_3$ exhibits an oxide ionic conductivity that is comparable with that of $La_{0.9}Sr_{0.1}Ga_{0.8}Mg_{0.2}O_3$.[29] In addition, the activation energy for ion conductivity in Mn-doped sample is much smaller than that of Mg-doped ones. However, the small activation energy may suggest the dominant electronic conduction in this oxide. In contrast, the total conductivity of Fe- or Co-doped specimens is almost independent of the oxygen partial pressure. This suggests that the oxide ion conductivity increases by doping Co or Fe.[30] Therefore, the oxide ion conductivity in Co-doped $LaGaO_3$-based oxide will be important.

Figure 14 shows the electrical conductivity of Co-doped LSGM at 1273 K, $P_{O2} = 10^{-5}$ atm and the transport number of oxide ion at 1273 K as a function of Co content. The electrical conductivity increases, whereas the transport number of oxide ion decreases with increasing amount of Co. The oxide ion conductivity values estimated from the transport number and the total conductivity are shown in Fig. 15. The electrical conductivity became higher with increasing amount of doped Co and attains a maximum value around 10 mol %. The appa-

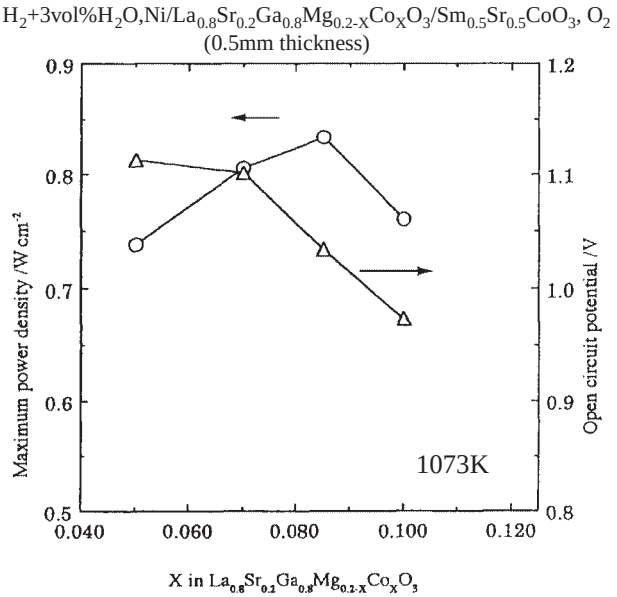

Fig. 16. Open circuit potential as well as the maximum power density at 1073 K as a function of Co content in $LaGaO_3$-based oxide electrolyte.

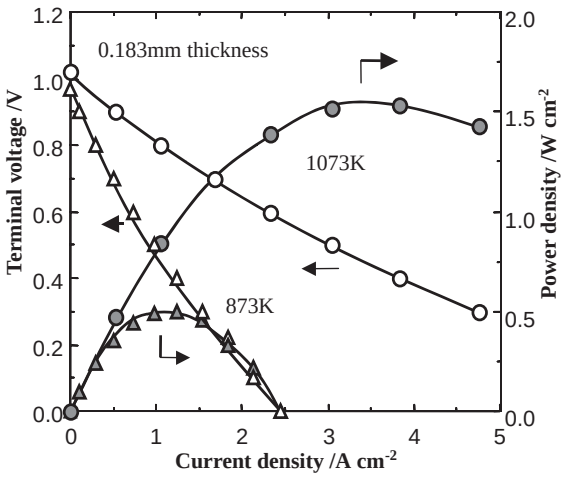

Fig. 17. Power generating property of H_2–O_2 cell at 1073 and 873 K using 0.18 mm thickness LSGMC-8.5 for the electrolyte.

rent activation energy for the electronic conduction monotonically decreased with increasing Co concentration and reaches a value of 0.45 eV for 10 mol % Co, which is almost half of the value reported for YSZ. Although the highest oxide ion conductivity is obtained at $X = 0.1$, the transport number of oxide ion becomes smaller than 0.9. Since the decreased transport number of oxide ion leads to a decrease in the energy conversion efficiency of SOFC, it is considered that the desirable composition as the electrolyte for SOFC is $La_{0.8}Sr_{0.2}Ga_{0.8}Mg_{0.115}Co_{0.085}O_3$ (denoted as LSGMC-8.5) or one with even lower Co content.

Figure 8 also shows the comparison of oxide ion conductivity of Co-doped $LaGaO_3$-based oxide with the conventional oxide ion conductivity values. It is seen that Co-doped $LaGaO_3$-based oxide exhibits even higher conductivity than that of LSGM and Gd-doped CeO_2. The values are close to that of Bi_2O_3-based oxide, which exhibits pure oxide ion conduction in a limited P_{O2} range. Therefore, Co-doped $LaGaO_3$, in particular LSGMC-8.5, is highly attractive to use as the the electrolyte of a solid oxide fuel cell.

Figure 16 shows the open circuit potential as well as the maximum power density at 1073 K as a function of Co content in $LaGaO_3$-based oxide electrolyte.[31] The open circuit potential (OCV) decreases monotonically with increasing Co amount. In particular, decrease in OCV is significant when Co content is higher than 10 mol % in Ga site. This is caused by the appearance of the hole conduction due to doping Co. The dependence of OCV on the amount of doped Co is in good agreement with that of the transport number of oxide ion, as shown in Fig. 15. On the other hand, the power density increased with increasing Co content and it attained a maximum value at 8.5 mol % of Co doped for Ga sites. Improvement in the power density is simply explained by the improved oxide ion conductivity due to doping Co. When the amount of doped Co became excessive, the hole conduction becomes significant and the cell becomes short-circuited, resulting in a decrease in the power density. Consequently, it is obvious that the maximum power density is obtained at 8.5 mol % Co-doped LSGM for electrolyte.

On the other hand, it is expected that the power density of the cell increased with decreasing thickness of the electrolyte, since the main internal resistance is still IR loss. Figure 17 shows the power density of H_2–O_2 cell using 0.18 mm thickness LSGMC-8.5 for the electrolyte at 1073 and 873 K. As expected, the power density of the cell increases with decreasing the thickness of the LSGMC electrolyte. However, the open circuit potential exhibited a tendency to decrease with decreasing the thickness of electrolyte. This is explained by the increased amount of leaked oxygen with decreasing thickness, since LSGMC exhibits a small hole conduction. At 0.18 mm electrolyte thickness, as shown in Fig. 17, the open circuit potential decreased to 0.94 V at 873 K. Therefore, from the conversion efficiency point of view, it is expected that the desirable thickness will exist. However, it is obvious that an extremely large power density is attained for thinner electrolytes. The maximum power density is attained to values of 1.58 and 0.50 W cm^{-2} at 1073 and 873 K, respectively, as shown in Fig. 17. This power density at 873 K suggests that an SOFC operable at less than 873 K can be realized by using a LSGMC thin film as an electrolyte. The electronic power generation property of an even larger-sized cell (ϕ150 mm) using $La_{0.8}Sr_{0.2}Ga_{0.8}Mg_{0.15}Co_{0.05}O_3$ is also reported recently.[32,33] Based on the high power density of the cell using LSGMC for an electrolyte, stacking of the cells using LSGMC electrolyte was developed under collaboration with Mitsubishi Materials and Kansai Electric Power Co. Figure 18 shows the cell design used for the stacking cell. Since one of the great drawbacks of the SOFC stack is the gas seal, we adopted a so-called seal-less structure. Both fuel and air were fed at the center of a cylindrical cell and uncombustible fuel was oxidized at the outer part of the cell module. Figure 19 shows the power generating property of the cells used for stacking, which were prepared by tape-casting method. It is seen that the prepared cell also exhibits a high power density at larger cell size of

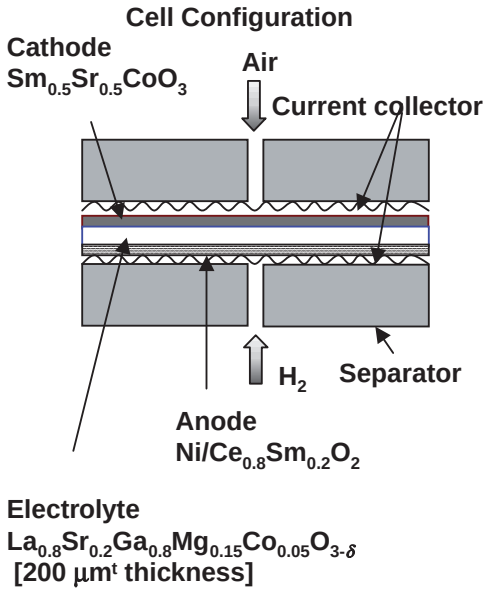

Fig. 18. Schematic view of the cell design used for stacking cell under collaboration with Mitsubishi Materials and Kansai Electric Power Company.

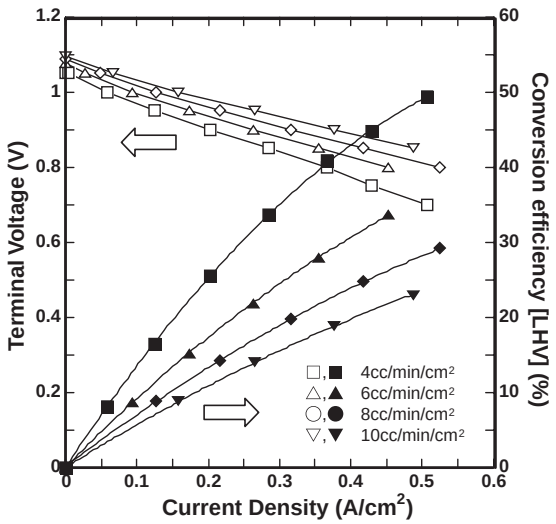

Fig. 19. Power generating property of the cell used for stacking cell.

ϕ40 mm comparing with that of our studied one (ϕ20 mm). The power density can reach a value of 0.2 W cm^{-2} at a terminal potential of 0.7 V. It is also noted that the energy conversion efficiency was close to 50% (LHV) at 973 K. Therefore, high energy conversion efficiency could be expected on the SOFC using LSGMC electrolyte. Figure 20 shows the SOFC system developed recently by Mitsubishi Materials by using LSGMC electrolyte. This system successfully demonstrated the total power of 1 kW, as expected and shows a small degradation rate during 1500 h operation. These data suggest that the developed $LaGaO_3$-based oxide is highly promising as the oxide ion conductor for lowering the temperature operation of SOFC. This collaboration work is now containing and the current target size of the cell module is 10 kW, which will be achieved during the following few years.

Fig. 20. SOFC system developed recently by Mitsubishi Materials by using LSGMC electrolyte.

6. Preparation of $LaGaO_3$ Thin Film and Applied for SOFC Operable at less than 773 K

Although the operating temperature of the SOFC could be lowered by using LSGMC electrolyte, an operating temperature of 973 K is still high for the mobile application and further decrease in operating temperature is still required by industry. However, further decrease in operating temperature can be expected by using $LaGaO_3$ thin films. In this section, preparation of LSGM film was described and the power generating performance of the cell using the resulting LSGM thin film was introduced.

Many efforts have recently been made to fabricate SOFC single cell with LSGM thin film as electrolyte.[34–36] Because of the reaction between LSGM and NiO during fabrication of the cell, the high performance of the cell is not available by using LSGM film.[34,35] On the other hand, for SOFC applications, electrolyte films were normally prepared directly on the porous substrates. If a porous substrate is employed, the thickness of the electrolyte film will be limited to a relatively large value like 30–50 μm. However, a much thinner electrolyte film (<5 μm) can be easily fabricated on the dense substrate. Therefore, in this study, we developed a new concept for preparation of thin $LaGaO_3$-based oxide film for the intermediate temperature SOFC.[37] The dense anode substrate was used for fabrication of a thin LSGM film as electrolyte by pulsed laser deposition (PLD). In order to prevent the reaction between substrate and electrolyte, SDC thin film was introduced between LSGM and NiO–Fe_3O_4–SDC substrate. The introduction of a small amount of iron oxide into nickel oxide can increase the chemical compatibility between LSGM and NiO and can lower the anodic overpotential. Since NiO and Fe_3O_4 were reduced to Ni and Fe by H_2 treatment, the dense substrate was changed to a porous one and can be used as a porous anode substrate for SOFC.

The deposition parameters and the composition of the target were optimized to get a dense electrolyte film with stoichiometric composition. The laser power and frequency were controlled at 180 mJ pulse^{-1} and 10 Hz, respectively. The sub-

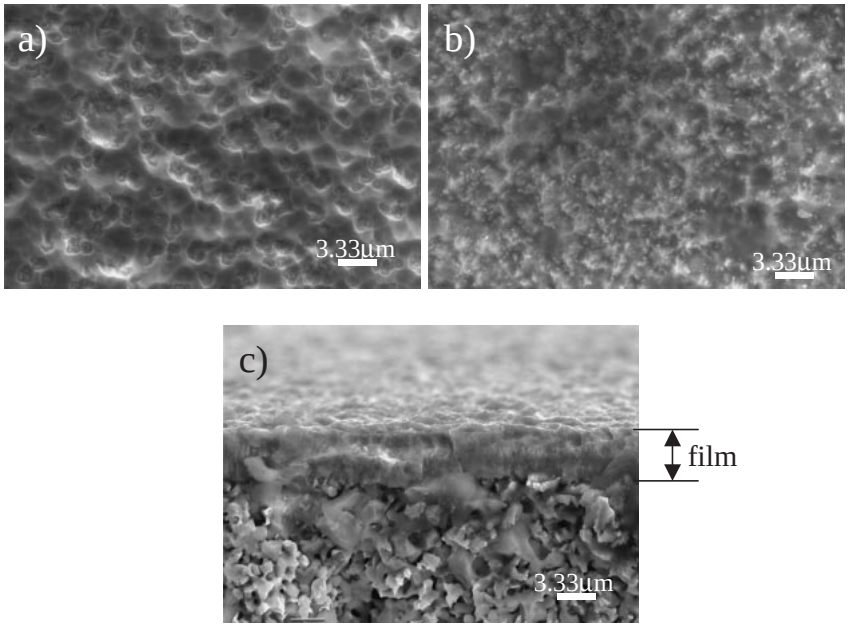

Fig. 21. Surface morphology and the cross view of LSGM/SDC composite film prepared by pulsed laser ablation method. a) As-deposited, b) after post annealed, and c) cross view after reduction.

strate was heated to 1073 K by an infrared heater and the background pressure of oxygen was adjusted to 0.005 Pa. In order to facilitate the electrode process, firstly a thin layer of $Ce_{0.8}Sm_{0.2}O_{2-\delta}$ (SDC, ca. 400 nm) was deposited on the anode substrate, and then LSGM film (ca. 5 μm) was deposited. Both resulting LSGM and SDC film were confirmed by EDX to be almost the same as those of the target one. XRD analysis revealed that the perovskite phase of LSGM was formed in the thin film after deposition. The samples were post-annealed in air at 1073 K for 60 min to ensure the superior contact and development of the crystal structure of LSGM.

Figure 21 shows the surface morphology and the cross view of LSGM/SDC composite film before and after annealing treatment. No pinholes or cracks formed on the surface of the as-deposited and post-annealed films. The surface of the as-deposited film was smoother than that of the annealed one. On the surfaces of both films, no obvious grain boundaries can be observed. The LSGM/SDC composite film was dense and uniform in thickness, as shown in Fig. 21c. Although the substrate became porous after the in-situ reduction of anode substrate, the electrolyte film still kept gas-tightness, indicating that the strength of the LSGM/SDC film is high enough and that the change in size of the anode substrate is not large during the reduction. Results also suggested that the thermal expansion coefficient of the LSGM/SDC composite film matches well with that of the anode substrate prepared.

The power generating property of the SOFC single cell using $Sm_{0.5}Sr_{0.5}CoO_3$ as cathode is shown in Fig. 22. Because LSGM/SDC thin film was utilized as electrolyte in this cell, high maximum power density was expected. So the cell was only operated at relatively low temperatures from 673 to 973 K. The open circuit voltage (OCV) at 973 K reached a value of 1.08 V, which is close to the theoretical electromotive force (1.15 V) for a H_2–O_2 SOFC single cell under the used condition. So the LSGM/SDC composite film was dense,

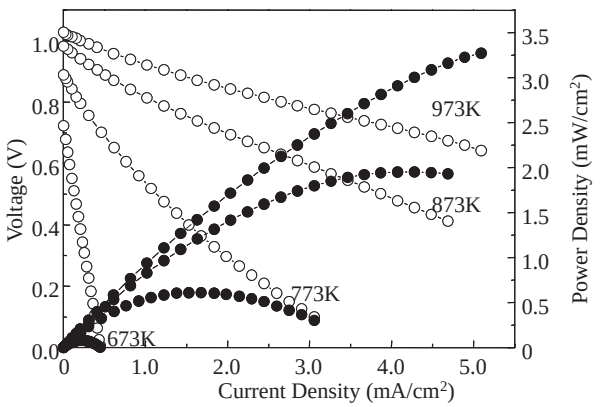

Fig. 22. Power generating property of the SOFC single cell using $Sm_{0.5}Sr_{0.5}CoO_3$ as cathode.

i.e., gas-tightness. With lowering the operation temperature, the OCV gradually decreased. Gas leakage from the molten Pyrex glass seal may lead to this phenomenon. Although the porosity of the anode substrate was not so high compared with that of the normal anode on electrolyte plate, it is interesting that no concentration polarization was observed on the *I*–*V* curves even though very high current flowed through the anode substrate. That means H_2 can be easily permeated through the anode substrate. The maximum power density of this cell reached values of 3270, 1951, 612, and 80 mW cm^{-2} at 973, 873, 773, and 673 K, respectively. This is the highest power density for double chamber SOFC single cells reported in the open literature. This result indicates that the thin film SOFC can be operated at temperature lower than 773 K with a reasonably high power density. Successful demonstration of a thin film SOFC single cell with high power density at reduced temperatures (from 673–873 K) may expand the SOFC application to mobile power area.

7. Concluding Remarks

In this study, the current status of the promising oxide ion conductors of $LaGaO_3$-based oxide for the electrolyte of SOFC is introduced. Large part of such non-fluorite oxide ion conductors has the cubic-like perovskite structure. Recently, there are some reports on such new oxide ion conductors. Some of the non-cubic oxide conductors such as $La_{10}Si_6O_{27}$ or La_2GeO_5 are highly interesting. Therefore, in some near future, there is a high possibility that the new non-cubic oxide exhibiting extremely fast ion conductivity will be found. At present, the electrolyte for high-temperature SOFC, which is operating around 1273 K, seems to be fixed at Y_2O_3-stabilized ZrO_2; however, one for the intermediate temperature has not been determined yet. The most promising candidate of electrolyte at the time of writing is considered to be $LaGaO_3$-based oxide which was found by our group. On the other hand, if the operating temperature can decrease to the range from 673–873 K, development of SOFC for the practical use could be accelerated greatly. Such intermediate temperature fuel cells (ITFC) will open a new application area for fuel cells, since the power generating system should be the simplest among the all types of fuel cells. In this ITFC, hydrocarbon fuels can be directly used (no pre-reformer). Gas seal also became much easier comparing with the high-temperature one. For realizing the SOFC operating less than 773 K, one must overcome many subjects overcome; however, we consider that the day when SOFC is operable at such low-temperature ranges is not so far in the future. We hope that the $LaGaO_3$ could open a such new field of SOFC.

References

1 T. Ishihara, N. M. Sammes, O. Yamamoto, *High Temperature Solid Oxide Fuel Cells: Fundamentals, Design, and Applications*, Elsevier, **2003**, Chap. 4, pp. 83–117.

2 T. Ishihara, H. Arikawa, T. Akbay, H. Nishiguchi, Y. Takita, *J. Am. Chem. Soc.* **2001**, *123*, 203.

3 S. Nakayama, M. Sakamoto, *J. Eur. Ceram. Soc.* **1998**, *18*, 1413.

4 S. Nakayama, *Mater. Integr.* **1999**, *12*, 57.

5 M. O'Connell, A. K. Norman, C. F. Hüttermann, M. A. Morris, *Catal. Today* **1999**, *47*, 123.

6 T. Takahashi, H. Iwahara, *Energy Convers.* **1971**, *11*, 105.

7 M. Cherry, M. S. Islam, C. R. A. Catlow, *J. Solid State Chem.* **1995**, *118*, 125.

8 T. Ishihara, H. Matsuda, Y. Takita, *J. Electrochem. Soc.* **1994**, *141*, 3444.

9 T. Ishihara, H. Matsuda, Y. Mizuhara, Y. Takita, *Solid State Ionics* **1994**, *70/71*, 234.

10 T. Ishihara, H. Matsuda, Y. Takita, Proceedings 2nd Ionic and Mixed Conducting Ceramics, Electrochemical Society, **1994**, p. 85.

11 T. Ishihara, H. Matsuda, Y. Takita, *J. Am. Chem. Soc.* **1994**, *116*, 3801.

12 P. Majewski, M. Rozumek, F. Aldinger, *J. Alloys Compd.* **2001**, *329*, 253.

13 T. Ishihara, H. Matsuda, Y. Takita, *Solid State Ionics* **1995**, *79*, 147.

14 M. Feng, J. B. Goodenough, *Eur. J. Solid State Inorg. Chem.* **1994**, *31*, 663.

15 P. N. Huang, P. Petric, *J. Electrochem. Soc.* **1996**, *143*, 1644.

16 K. Huang, R. Tichy, J. B. Goodenough, *J. Am. Ceram. Soc.* **1998**, *81*, 2565.

17 R. T. Baker, B. Gharbage, F. M. B. Marques, *J. Electrochem. Soc.* **1997**, *144*, 3130.

18 K. Yamaji, T. Horita, M. Ishikawa, N. Sakai, H. Yokokawa, M. Dokiya, *SOFC V*, Electrochemical Society, **1997**, Proc. Vol. 97-18, p. 1041.

19 J. H. Kim, H. I. Yoo, *Solid State Ionics* **2001**, *140*, 105.

20 H. Yokokawa, N. Sakai, T. Horita, K. Yamaji, *Fuel Cell* **2001**, *1*, 117.

21 K. Huang, J. H. Wan, J. B. Goodenough, *J. Electrochem. Soc.* **2001**, *148*, A788.

22 K. Huang, M. Feng, J. B. Goodenough, M. Schmerling, *J. Electrochem. Soc.* **1996**, *143*, 3630.

23 K. Yamaji, T. Horita, M. Ishikawa, N. Sakai, H. Yokokawa, *Solid State Ionics* **1998**, *108*, 415.

24 H. Hayashi, M. Suzuki, H. Inaba, *Solid State Ionics* **2000**, *128*, 131.

25 T. Ishihara, J. A. Kilner, M. Honda, Y. Takita, *J. Am. Chem. Soc.* **1997**, *119*, 2747.

26 T. Ishihara, H. Furutani, M. Honda, T. Yamada, T. Shibayama, T. Akbay, N. Sakai, H. Yokokawa, Y. Takita, *Chem. Mater.* **1999**, *11*, 2081.

27 R. T. Baker, B. Gharbage, F. M. B. Marques, *J. Electrochem. Soc.* **1997**, *144*, 3130.

28 V. V. Kharton, A. A. Yaremchenko, A. V. Kovalevsky, A. P. Viskup, E. N. Naumovich, P. E. Kerko, *J. Membr. Sci.* **1999**, *163*, 307.

29 V. Thangadurai, A. K. Shukla, J. Gopalakrishnan, *Chem. Commun.* **1998**, 2647.

30 T. Ishihara, T. Shibayama, M. Honda, H. Nishiguchi, Y. Takita, *J. Electrochem. Soc.* **2000**, *147*, 1322.

31 T. Ishihara, T. Shibayama, M. Honda, H. Nishiguchi, Y. Takita, *Chem. Commun.* **1999**, 1227.

32 J. Akikusa, K. Adachi, K. Hoshino, T. Ishihara, Y. Takita, *J. Electrochem. Soc.* **2001**, *148*, A1275.

33 T. Yamada, N. Chitose, J. Akikusa, N. Murakami, T. Akbay, T. Miyazawa, K. Adachi, A. Hasegawa, M. Yamada, K. Hoshino, K. Hosoi, N. Komada, H. Yoshida, M. Kawano, T. Sasaki, T. Inagaki, K. Miura, T. Ishihara, Y. Takita, *J. Electrochem. Soc.* **2004**, *148*, A1712.

34 M. Sahibzada, B. C. H. Steele, D. Barth, R. A. Rudkin, I. S. Metcalfe, *Fuel* **1999**, *78*, 639.

35 J. W. Yan, Z. G. Lu, Y. Jiang, Y. L. Dong, Y. C. Yu, W. Z. Li, *J. Electrochem. Soc.* **2002**, *149*, A1132.

36 Z. H. Bi, B. L. Yi, Z. W. Wang, Y. L. Dong, H. J. Wu, Y. C. She, M. J. Cheng, *Electrochem. Solid-State Lett.* **2004**, *7*, A105.

37 J. Yan, H. Matsumoto, M. Enoki, T. Ishihara, *Electrochem. Solid-State Lett.* **2005**, *8*, A389.

Tatsumi Ishihara was born in 1961 in Okayama and received his Dr. of Engineering degree from Kyushu University in 1991. In 1986, he received his M.Sc. from Kyushu University and then joined the Graduate school of Science and Technology as a research associate. He moved to the Faculty of Engineering, Oita University in 1989 and he was promoted to lecturer in 1990 and to associate professor in 1991. He became a professor in the Faculty of Engineering, Kyushu University in 2003. His main subjects include the inorganic functional materials and catalysts, in particular, materials related with solid oxide fuel cells and electrochemical devices. He received The Chemical Society of Japan Award for Young Chemists in 1995, the Petroleum Society Japan in 1998, and the Catalysis Society of Japan in 1999. He was also awarded The Chemical Society of Japan Award for Creative Work in 2004.